

RSC Advances



This is an *Accepted Manuscript*, which has been through the Royal Society of Chemistry peer review process and has been accepted for publication.

Accepted Manuscripts are published online shortly after acceptance, before technical editing, formatting and proof reading. Using this free service, authors can make their results available to the community, in citable form, before we publish the edited article. This *Accepted Manuscript* will be replaced by the edited, formatted and paginated article as soon as this is available.

You can find more information about *Accepted Manuscripts* in the [Information for Authors](#).

Please note that technical editing may introduce minor changes to the text and/or graphics, which may alter content. The journal's standard [Terms & Conditions](#) and the [Ethical guidelines](#) still apply. In no event shall the Royal Society of Chemistry be held responsible for any errors or omissions in this *Accepted Manuscript* or any consequences arising from the use of any information it contains.



Journal Name

ARTICLE

A microfluidic chip for high resolution Raman imaging of biological cells

Received 00th January 20xx,
Accepted 00th January 20xx

Barbara M. Liszka^a, Hoon Suk Rho^b, Yoon Sun Yang^a, Aufried T.M. Lenferink^a, Leon W.M.M. Terstappen^a, Cees Otto^a

DOI: 10.1039/x0xx00000x

www.rsc.org/

A microfluidic chip was designed, prepared and tested for integration with a confocal Raman imaging spectrometer with the special purpose to enable studies of individual biological cells. The design of the chip effectively overcomes the limitations arising from high numerical aperture (NA) and short working distance objectives which are necessary for high resolution imaging. The high confocal spatial resolution was achieved by a careful design of the geometry of the chip together with thin, optically and Raman silent sealing window as the embedding medium for the channels. A leak-free microfluidic chip was obtained by surface plasma modification of polydimethylsiloxane (PDMS), and optimization of liquid loading parameters. Raman images of biological cell, which were transported by flow into the microfluidic chip, are presented as an example of Raman-microfluidics application. The broad band Raman spectra from -50 cm^{-1} to 3650 cm^{-1} were recorded in 1600 frequency intervals without any signal enhancement or sample labeling. Raman images were recorded in ~ 400 seconds and typically consist of 64×64 pixels with a step size of 250 nm thus all together containing $\sim 4 \times 10^6$ data points.

Introduction

Microfluidic platforms are well-known devices that enable precise handling of liquids and flow manipulation of multiple compounds in reaction chambers.¹ The advantages of microfluidics are a significant sample volume reduction, portability, automation and hazard control. Raman microscopy can be used in microfluidic devices as it is possible to acquire spectra from very small volumes ($< 1\text{ pL}$). Raman microscopy is a spectroscopic light scattering technique which provides image contrast based on the differences in amplitude energy of light scattering of vibrational states, which are characteristic for specific molecular bonds. Raman spectra represent a "fingerprint" of a chemical compound by which the compound can be identified without labeling. The method is non-destructive and compatible with measurements in aqueous environment because the Raman light scattering of water is relatively weak. Moreover, it offers high spatial resolution, common to optical microscopy, and high optical sensitivity due to high signal collection efficiency. The confocal Raman microscope system enables to target specific areas in a sample, therefore a high discrimination between the sample of interest and other materials in the immediate surroundings of the sample can be achieved.² Due

to the aforementioned aspects, integration of both techniques is an attractive tool in fields such as: chemistry, in-vitro diagnostic and biotechnology.^{3, 4} It has been shown that microfluidic platforms integrated with a Raman spectrometer set-up can be applied for various analytical purposes² such as imaging of two liquid mixing,⁵ imaging of mixing profile,^{6, 7} measuring the concentration output,⁸ bio-fluid analysis,⁹ *in situ* spectral imaging of biofilms under dynamic flow,¹⁰ and monitoring various chemical reactions,^{10-12, 13}. Another application of imaging in microfluidics under spectroscopic conditions is a flow-through microarray cell for online detection of E-coli bacteria.¹⁴

Surface Enhanced Raman Spectroscopy (SERS)¹⁵ integrated with microfluidics is most often reported because the Raman signal is enhanced up to 10^8 fold,¹⁶ which efficiently overcomes the undesired Raman scattering from the surroundings. Nevertheless, the method requires metallic structures either on a surface or in a colloidal solution, which limits the analysis to chemicals, which can be immobilized on a nanostructured metal. In addition, quantitative analysis is not possible in a direct way as an inhomogeneous distribution of nanoparticles cannot be excluded. SERS images of a single living cell in a microfluidic devices have been reported independently by Zhang *et al.*¹⁷ and Syme *et al.*¹⁸, with a contrast dominated by the response of the enhancing nanoparticles and not by the cells. Spontaneous Raman Spectroscopy is a label free method but imaging of biological cells is challenging due to the weak Raman signal. It can be even more problematic in microfluidic chips, which introduces significant background noise of substrates such as PDMS, silicon or glass. In addition, the working distance of the objective must be long enough to acquire images inside a microfluidic chip. Microfluidic chips have usually several millimeters of thickness, which makes it compatible with long working distance

^a Department of Medical Cell BioPhysics, MIRA institute, University of Twente Enschede, The Netherlands,

^b Department of Mesoscale Chemical System, MESA+ institute, University of Twente Enschede, The Netherlands
DOI: 10.1039/x0xx00000x

objectives. The low detection volume in microfluidic chips requires the optimization of focal depth and spot size to ensure that the Raman signal arises from the targeted voxel. Resolution of images is determined by numerical aperture of the objective, and in general decreases with a longer working distance. Application of a high NA objective results in better beam focusing and an increase in the signal to noise ratio. The depth of focus can be decreased by confocal mode.²

We have shown for the first time that high-resolution images can be acquired in a microfluidic chip by spontaneous Raman Spectroscopy. This is illustrated by high-resolution images of a cell. The images were obtained with a spatial resolution of 400 nm in the x and y direction and 1500 nm in the "z" direction with the step size 0.23 μm , with a total scan time of less than 7 minutes.

Materials and methods

Microfluidic chip fabrication and operation

The microfluidic chip was fabricated by standard soft lithography technique¹⁹. Mask design was prepared with CleWin software (MESA+, University of Twente) and printed on a 5 soda lime glass by mask generator LBP Heidelberg DWL200 (Heidelberg Instruments Mikrotechnik GmbH). By using the photoresist-based photolithographic techniques, we fabricated a master mold. Positive photoresist (AZ 40 XT, MicroChem Corp.) was spin-coated onto a 4" silicon wafer. Then, the coated wafer was exposed to UV light through masks and developed. Uncured PDMS (RTV 615, GE Silicones, Inc.; elastomer: cross-linker = 7:1) was poured onto the mold and cured for 45 minutes at 80 °C. The PDMS layer was peeled off from the mold and holes for inlet and outlet were punched with a 28-gauge punch (Syneo Co., Angleton, TX). The Raman grade calcium fluoride windows (CaF_2) (Crystran Ltd., UK) or quartz windows (Laser Optex In.) with a thickness of 200 μm was cleaned with ethanol. Next, the window was covered with 0.01 % poly-L-lysine (Sigma Aldrich) and left for 30 min at 37 °C, washed with milli-Q water and left to dry out. The chip was treated with oxygen plasma (for 30 s) to obtain hydrophilic surface and increase bonding strength between disk and PDMS. The microfluidics was sealed against a glass slide, which contained drilled-slots for the tubing connections to inlet and outlet.

Confocal Raman set-up

A microfluidic chip was integrated with a custom-built confocal Raman micro-spectrometer.²⁰ The set-up contains a Kr-ion laser (Coherent, Innova 90-K, Santa Clara, CA) with an excitation wavelength of 647.089 nm. An objective (40 x/ 0.95 NA, Olympus UplanSApo) was used to focus the light on the sample. The scattered light was collected by the same objective and transmitted through the dichroic beam splitter. The reflection of the laser light and elastic scattered photons were passed through an edge long pass filter. The scattered Raman light was focused on a confocal pinhole with a diameter of 15 μm , which functioned as the entrance aperture to the spectrograph. The spectrograph dispersed the light in the range from 646 to 849 nm. The Raman signal was detected by a 1600 x 200 pixel back illuminated CCD camera (Newton DU-970N-BV; Andor Technology). The combination of spectrograph and CCD camera in the setup records Raman shifts between -50 cm^{-1} and 3650 cm^{-1} .

Confocal Raman imaging and data analysis

Raman imaging was performed by stepping the laser beam over the region of interest. The cells were scanned over an area of 15 μm x 15 μm with a step size of 234 nm. Raman maps of 64 x 64 spectra over this area were acquired with an acquisition time of 0.1 s per

pixel. A z-scan of the microfluidic chip was performed by acquiring single Raman spectra at every step. The laser position was changed by moving a Piezosystems Jena (PZ400) nano stage using a NV 40/CL-E controller. Measurements were performed with a laser power under the objective of 35 mW.

The raw Raman spectra were corrected for: 1) cosmic ray events, 2) wavelength-dependence of the sensitivity of the complete Raman spectrometer, 3) CCD camera-etaloning and absolute amplitude correction by a calibrated light source. The combined output of a tungsten halogen lamp and the recorded Raman spectrum of toluene was used to convert pixels to wavenumbers. Singular value decomposition (SVD) was applied for the Raman data to improve the signal to noise ratio.²¹ Multivariate analysis containing hierarchical cluster analysis (HCA) and principal component analysis (PCA) were performed to visualize the regions of high spectral similarities.²²

Cell incubation in a microfluidic chip

Cells from the breast cancer cell line NCI-H1650 (ATCC, Manassas, VA, USA) were cultured at 37 °C in cell culture medium using an incubator which maintained an atmosphere of 95 % humidity and 5 % partial pressure of CO_2 . Cells were harvested 0.05% Trypsin-EDTA (Gibco). The cell suspension was injected into the microfluidic chip and left for 40 min up-side down to allow cells to sediment on the quartz surface and adhere. After this time the microfluidic chip was placed under the objective in such a way that the quartz disk was at the top.

Results

Microfluidics design for high resolution imaging

Polydimethylsiloxane (PDMS) was selected as a material for the microfluidic chip to produce an optically transparent device.¹ A calcium fluoride (CaF_2) or quartz window, with a thickness of 200 μm was used to seal the PDMS layer of the chip. The low thickness of the window enables the use of an objective with a 280 μm short working distance and a high numerical aperture (NA 0.95), (40X). This enabled the acquisition of high-resolution images from the inside of the fluidic channel. A schematic representation of the relation between spot size, depth of field, focal length and detection volume is presented in Figure 1A. Calcium fluoride (CaF_2)/quartz window were chosen as cell substrates to reduce the spurious background signal in Raman spectra, which would otherwise decrease the signal-to-noise ratio. The schematic representation of the cross section of the chip and a comparison of Raman spectra of both materials and glass is presented in Figure 1A and 1B respectively. It can be noticed (Figure 1B) that the light amplitude, which could consist of Raman scattering and/or fluorescence emission, that contributes to a non-informative background of CaF_2 and quartz is significantly lower than glass, which is essential for an optimal signal-to-noise ratio in Raman signal detection. Although the optical background of CaF_2 is lower than that of quartz, quartz windows can be sealed to the PDMS surface more strongly than CaF_2 after modification of the PDMS surface by a plasma oxidation process. A stronger bonding lowers the chance of leakage and liquid evaporation. A quartz substrate has a sufficiently low background (Figure 1B) and is a suitable window material for measurement of cells. CaF_2 windows can also be sealed with the same plasma-modification of the PDMS surface and no leakage occurs when aqueous solution was loaded with an over pressure up to 0.1 bar (results not shown). Here we show results when the microfluidics is sealed with a quartz window in combination with cell measurements.

The quartz window was coated with poly-L-lysine to avoid cell movement during Raman measurements.²³ The cell adhesion to the window is weak, therefore the exchange of medium or the addition of additional compounds into the reaction chamber must be performed under low pressure. The microfluidic chip has been designed to integrate with a Raman confocal microscope without changes to the set-up. The device was positioned on a standard microscope table with no hindrance to the microscope condenser. The pressure controller enables to load the channels and Raman images can be acquired under a controlled flow speed. A schematic representation of the device is presented in Figure 2.

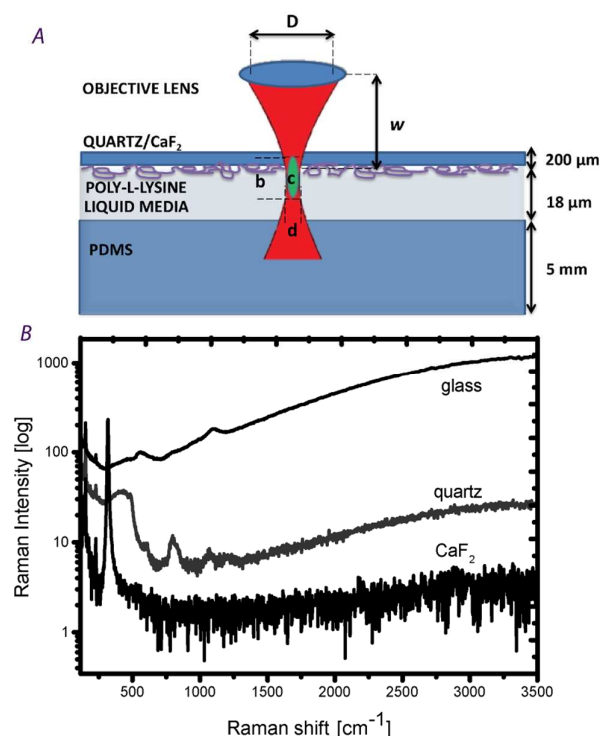


Figure 1A: Schematic representation of signal collection in microfluidic device during imaging. The side view of the device shows the order and dimensions of the layers. The figure schematically shows the focused laser beam (red) and the confocal sampling volume (green), characterized by *d*- lateral diameter of ~ 400 nm and *b*- an axial diameter of 1500 nm. *w*- is the working distance of the high NA objective of ~ 280 μm , and *D* is the lens diameter. **1B** A comparison of Raman spectra of calcium fluoride, glass and quartz shows the difference in background on a logarithmic intensity scale. The superior performance of CaF_2 is apparent.

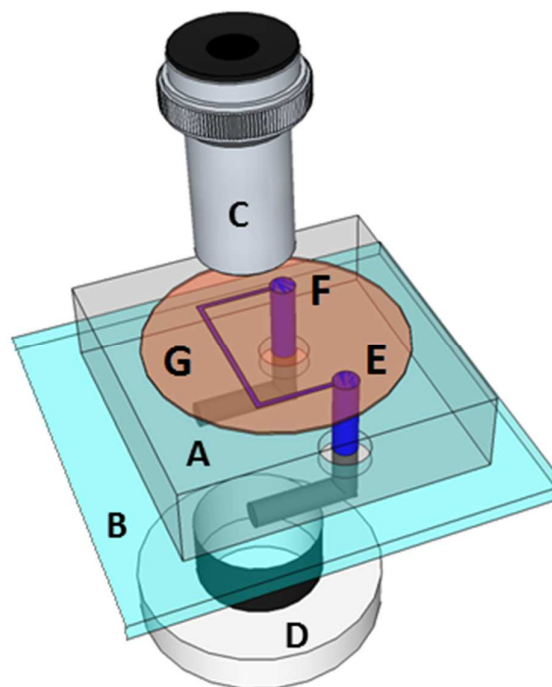


Figure 2 Three dimensional schematic of a microfluidic chip integrated with a Raman microscope. A chip (A) sealed to a glass slide (B) with input and output ports (E and F), placed in between an objective (C) and condenser (D). The top part of the chip contains a system of channels and valves covered with $\text{CaF}_2/\text{quartz}$ (G)

Raman z-scan through the microfluidic device.

The high surface to volume ratio in a microfluidic chip may cause a non-desirable background-noise in a Raman data set. A “z-scan” through the microfluidic chip filled with water was made to show the influence of each component of the chip for the Raman spectra at each z-position through the chip. The Raman spectra of quartz, water and PDMS are clearly distinguishable and have been used to investigate the contribution of a layer to the confocal plane of interest. The Raman spectra in the z-scan were taken every 0.2 μm along 200 μm . The data are presented in Figure 3 as a change of Raman signal intensity at various depths, for the most prominent bands of PDMS at 488 cm^{-1} , water at 3300 - 3700 cm^{-1} and the laser reflection at 0 cm^{-1} . The data points in the graph are calculated integrals for each band. The position of the laser focus in the microfluidic chip is represented by the blue curve. This curve shows the expected high reflected intensity when the laser is focused at the interface of layers. The position of the layers in the chamber can be obtained in this manner. It also corresponds well, with the water band intensity, which has a maximum signal contribution in the middle of the chamber.

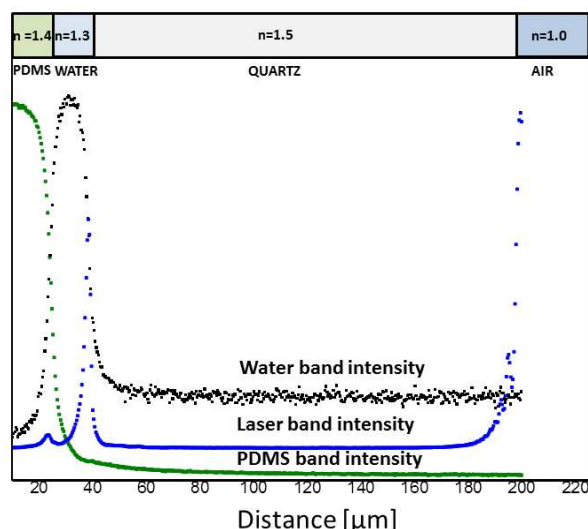


Figure 3. Comparison of the Raman signal intensity for selected bands of PDMS (488 cm^{-1} : green curve), water ($3300\text{--}3700\text{ cm}^{-1}$: black curve) and the laser reflection intensity (blue curve) through the microfluidic device. The top bar represents each layer and the corresponding refractive indexes in the microfluidic chip. The laser reflection (blue curve) maximizes at the interfaces. The curves for laser light intensity and water have been displaced for clarity.

The very intense Raman signal of PDMS drops rapidly and contributes weakly when the confocal plane coincides with the aqueous medium in the chamber. The focal volume is approximately a spheroid with a smaller-to-longer axis dimension of $400\text{ nm} \times 1500\text{ nm}$ whereas the height of the channel is $18\text{ }\mu\text{m}$. This distance is sufficient to decrease the intensity of the PDMS signal in the Raman spectrum of a cell adhered to the top window by about a factor of 10.

Cells in a microfluidic chip.

Raman images were acquired of single cells in a fluidic channel. The images were obtained by stepping the laser every 0.1 s with $0.234\text{ }\mu\text{m}$ over an area of $225\text{ }\mu\text{m}^2$, which resulted in 4096 spectra in less than 7 minutes. The white light image and the cluster image of the cell with corresponding color coded Raman spectra are presented in Figure 4. The nine cluster hierarchical cluster analysis (HCA) of the acquired Raman data set was performed. The images and corresponding average cluster Raman spectra shows that high-resolution images and high signal-to-noise ratio spectra can be acquired in the described microfluidic chip without any enhancement or labeling. The cluster Raman spectra present the composition of the cell in terms of important cellular compounds. Raman vibrations can be assigned to chemical compounds and groups, such as: 1002 (Phenylalanine), 1263 (amide III, collagen), 1300 (CH_2 twisting, protein, collagen), 1442 (cholesterol band), 1656 (amide I), 2852 (CH_2 symmetric stretch).²⁴ The background noise of PDMS and water is represented by the black cluster. Although, the intense Raman bands of PDMS, e.g. 610 cm^{-1} , 701 cm^{-1} , 1259 cm^{-1} , 1409 cm^{-1} contribute to the Raman spectra of the cell, the amplitude is low and has a minor negative contribution to the signal-to-noise ratio. The orange and brown, contains bands in position 1575 cm^{-1} and 1092 cm^{-1} which are characteristic for DNA.

These clusters represent the distribution of DNA in the nucleus. The red and dark green cluster spectrum show an intense band at 1442 cm^{-1} , assigned to cholesterol and lipid. The relative ratio in these two clusters varies and is strongly contrasted with the cell membrane (magenta), and the cytoplasm (light green). The violet cluster is distinguished from the cell membrane and envelops the entire cell to connect to the cytoplasm (light green). A univariate image of the cell is presented in Figure 4B. Each pixel represents the integrated Raman signal from position $1424\text{--}1473\text{ cm}^{-1}$, showing distribution of cholesterol, lipids and proteins in the cell. The bright green region corresponds to the red cluster in Figure 4C, which represents the highest concentration of cholesterol.

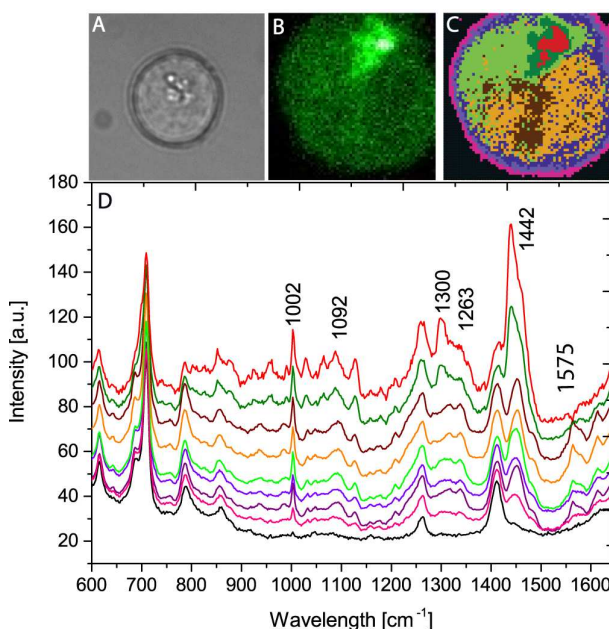


Figure 4. (A) The white light image of the cell in microfluidic channel through quartz window. (B) A univariate image of the cell from the Raman intensity in the region $1424\text{--}1473\text{ cm}^{-1}$. (C) 9 clusters image of the cell. The image size of $15\text{ }\mu\text{m} \times 15\text{ }\mu\text{m}$ was acquired with a step size of 234 nm , a time of 0.1 second per pixel and a laser power of 35 mW . (D) Color coded Raman cluster spectra are corresponding to the colors in the image. The spectra were shifted vertically for clarity.

Z-scans of the microfluidic chip were also acquired with a cell in the chamber. One z-scan was made through the cell and one z-scan was made next to the cell. Figure 5 compares the Raman signal intensity of the NCI-H1650 cell and PDMS along the z-coordinate for each selected confocal plane in the chip. The data points are integral intensities calculated for chosen bands (see Figure 4) for PDMS and the cell from the fingerprint region between 800 cm^{-1} and 1800 cm^{-1} . The spectral region for the cell does not overlap with the signal of the PDMS. The obtained results show that in the middle of the chamber the intensity of the PDMS signal is 4 times lower than that of the cell and it is \sim zero before the confocal plane reaches the quartz surface.

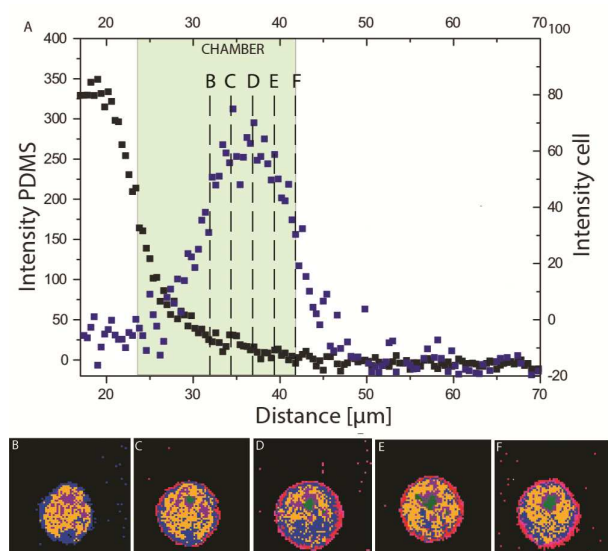


Figure 5 (A) Comparison of PDMS Raman signal intensity (black graph) and the cell in microfluidics (blue line). (B-F) The 10 clusters cell images acquired with the step size of 270 nm every 2.5 μm from the quartz surface. The image area: 30 μm X 30 μm , time 0.1 second per pixel, laser power 35 mW

In addition, images of the cell were acquired every 2.5 μm in the z-direction. Images based on hierarchical cluster analysis of the Raman data sets are presented in Figure 5 B-F. We have performed ten-level cluster analysis for each image which resulted in three clusters in image B and five clusters in images from F to C. Clusters that belong to the background are presented as one color (black) for better visibility of the cell. The variation in the background is due to varying contributions of PDMS, water and quartz at different depths in the microfluidics, as can be observed from the z-scan in Figure 5A. The cluster spectra connected to the cell distinguish variation in chemical composition and it can be directly observed that a different distribution occurs at different confocal depths. The image B, acquired 8 μm from the quartz surface, shows only the bottom part of the cell and therefore does not contain all clusters. The green cluster contains the most intense bands in positions: 1002 cm^{-1} (Phenylalanine), 1263 cm^{-1} (amide III, collagen), 1300 cm^{-1} (CH_2 twisting, protein, collagen), 1442 cm^{-1} (cholesterol) in comparison with the rest clusters. The green cluster spectrum shows bands at positions 1575 cm^{-1} and 1091 cm^{-1} which can be assigned to DNA. The results show 3D information of the chemical distribution in a single cell inside a microfluidic chip can be obtained.

Conclusion

We have designed, prepared and tested a microfluidic chip that enables acquisition of high-resolution Raman images of a biological cell in a chip for the first time. The chip was adapted to the stringent requirements of high NA objectives, which are essential in high resolution Raman and, in general, optical imaging. The microfluidic channels were embedded in PDMS, which has a strong

Raman spectrum that easily overwhelms information from biological cells. The careful design of the microfluidic chip together with a successful coupling to a confocal Raman micro spectrometer enables acquisition of high spatial resolution Raman images of cells in both 2D and 3D measurement mode. The expected contribution of Raman scattering from other materials in the chip, such as e.g. PDMS and quartz or CaF₂ has been minimized in this design. It was further shown that the chip can be filled with aqueous solution with or without cells without leakage, due to a sufficiently strong bonding of either CaF₂ or quartz to PDMS, by involving plasma treatment of PDMS and optimization of fluid loading parameters.

AUTHOR INFORMATION

B.M. Liszka; e-mail: b.liszka@utwente.nl, C. Otto: c.otto@utwente.

Notes and references

- D.C. Duffy, J. C. McDonald, O. J. A Schueller G. Whitesides, *Anal. Chem.*, 1998, **70**, 4974-4984.
- A. F. Chrimes, K. Khoshmanesh, P.R. Stoddart, A. Mitchell K.Kalantar-Zadeha, *Chem. Soc. Rev.*, 2013, **42**, 5880-5906.
- D.Janasek, J. Franzke, A. Manz, *Nature*, 2006, **422**, 374-380.
- W. Fritzsche, J.Popp J, *Optical Nano and Microsystems for Bioanalytics*, Springer, Berlin, 2012.
- A. A. Jean-Baptiste Salmon, Patrick Tabeing, *Appl. Phys. Lett.*, 2005, **86**.
- P. D. I .Fletcher, S. J. Haswell, X.Zhang, *Electrophoresis*, 2003, **24**, 3239-3245.
- A. E. Kamholz, E. A Schilling., P. Yager, *Biophys. J.*, 2001, **80**, 1967-1972.
- S.Leung, R. F. Winkle, R. C. R. Wootton, A. J. deMello, *Analyst*, 2005, **130**, 46-51.
- K. W. Kho, K. Z. M. Qing, Z. X. Shen, I. B. Ahmad, S. S. Lim, S. Mhaisalkar, T. J. White, F. Watt, K. C. Soo, M. Olivo, *J. Biomed. Opt.*, 2008, **13**, 054026.
- F. Paquet-Mercier, N. Aznavah, M. Safdar G. J., *Sensors* 2013, **13**, 14714-14727.
- A. J. deMello, *Nature*, 2006, **442**, 394-402.
- S.E. Barnes, Z. T. Cygan, J. K. Yates, L. Kathryn, E.J. Amis, B. Amis, *The Analyst*, 2006, **131**, 1027-1033.
- F. Sarrazin, J.B. Salmon, D. Talaga, L. Servant, *Anal. Chem.*, 2008, **80**, 1689-1695.
- M. Knauer, N. P. Ivleva, R. Niessner, C. Haisch, *Anal Bioanal. Chem.*, 2012, **402**, 2663-7
- M. Fleischmann, P. J. Hendra, A. J. McQuillan, *Chem. Phys. Lett.*, 1974, **26**.
- J. Kneipp, H. Kneipp, A. Rajadurai, R. W. Redmond, K. Kneipp, *J. Raman Spectrosc.*, 2009, **40**, 1-5.
- X. Zhang, H. Huabing, J.M. Cooper, S.J. Haswell, *Anal. Bioanal. Chem.*, 2008, **390**, 833-840.
- C. D. Syme, N. M. S. Sirimuthu, S. L. Faley, J. M. Cooper, *Chem. Commun.*, 2010, **46**, 7921-7923.
- Y. Xia, G. Whitesides, *Annual Review of Materials Science*, 1998, **28**, 153-184.
- V. V. Pully, A. Lenferink, C. Otto, *J. Raman Spectrosc.*, 2010, **41**, 599-608.

COMMUNICATION

Journal Name

21. N. Uzunbajakava, A. Lenferink, Y. Kraan, E. Volokhina, G. Vrensen, J. Greve and Otto C., *Biophys. J.*, 2003, **84**, 3968-3981.
22. N. Uzunbajakava., J. Greve C. Otto, *Multiphoton Microscopy in the Biomedical Sciences III*, 2003, 223-230.
23. D. Mazia, G. Schatten, W. Sale , *J. Cell Biol.*, 1975, **66**, 198-200.
24. Z. Movasaghi , S. Rehman, I. U. Rehman, *Appl. Spectrosc. Rev.*, 2007, **42**, 493-541.

Acknowledgment

This work is part of the research program "Spectroscopic analysis of particles in water", which is (partly) financed Fundamenteel Onderzoek der Materie (FOM), which is financially supported by the Nederlandse Organisatie voor Wetenschappelijk Onderzoek (NWO). This work was performed in the cooperation framework of Wetsus, Centre of Excellence for Sustainable Water Technology . Wetsus is co-funded by the Dutch Ministry of Economic Affairs and Ministry of Infrastructure and Environment, the European Union Regional Development Fund, the Province of Fryslân, and the Northern Netherlands Provinces.